J. Serafini, G. Bernardini, R. Porcelli, P. Masarati
In-Flight Health Monitoring of Helicopter Blades via Differential Analysis
Aerospace Science and Technology, Vol. 88, 2019, p. 436-443
doi:10.1016/j.ast.2019.03.039

In-flight health monitoring of helicopter blades via differential analysis

Jacopo Serafini[a], Giovanni Bernardini[a], Roberto Porcelli[a], Pierangelo Masarati[b]

[a] *Roma Tre University, Department of Engineering, Via della Vasca Navale, 79, 00144, Roma, Italy*
[b] *Politecnico di Milano, Department of Aerospace Science and Technology, Via Giuseppe La Masa, 34, 20156, Milano, Italy*

Abstract

This paper presents an original approach to structural health monitoring of helicopter rotors based on strain measurement on the blades. Three algorithms are presented, one in the time domain and two in the frequency domain. They are based on the analysis of the discrepancies between the strains on damaged and undamaged blades. Two damage types are considered: a mass unbalance at the tip, and a localized stiffness reduction. The performance of the proposed methods is assessed by numerical simulation using a multibody dynamic solver for comprehensive aeroelastic analysis of rotorcraft. The numerical investigation has highlighted the capability of all the presented techniques to detect damages in the blades, even of small entity, in both steady-flight and soft maneuvers. The reduced prediction accuracy in aggressive maneuvered flight suggests the use of these methods only in steady or quasi-steady flight conditions.

Keywords: Helicopter blades, strain gauges, in-flight health monitoring

1. Introduction

Helicopter rotor blades are subject to significant dynamic loads and deflections both in standard and critical operating conditions, owing to aerodynamics and inertia. They are slender flexible structures, whose flapping deformation is used both to direct rotor thrust (thus generating rolling and pitching moments) and to reduce aerodynamic asymmetry between the advancing and retreating

rotor blades. Furthermore, their flexibility allows to reduce the strong vibratory loads that would be transmitted to the airframe by rigid blades [1]. Damages on main rotor can lead to reduced performance or even catastrophic incidents, making it one of the most critical systems for the helicopter safety. In addition to the fatigue caused by periodic stresses, additional major threats to the integrity of modern composite blades include low-velocity impact, moist absorption, and progressive damage accumulation [2]. Currently, the rigid certification process envisages statistical fatigue evaluation and threat assessment for damage tolerance to exceptional events (e.g. CS 27.573 in [3]). In order to fulfill safety criteria, this approach requires high safety margins, both in terms of design/fabrication and inspections/maintenance. Furthermore, for certification purposes (e.g. CS 27.571 in [3]) in-flight rotor loads or stress measurements in all critical conditions are required. Anyway, many types of damage may be confused with unbalance, which is periodically cured by tracking. Low-velocity impacts may go unnoticed, especially if only minor external traces are present. Structural integrity is checked by mechanical means (e.g. "tapping") and, if needed, by non-destructive analysis. However, such types of analysis are usually expensive and time-consuming, implying some significant downtime of the helicopter. Except for detected low-velocity impacts, inspections occur according to specific schedules. The ability to determine the need of an inspection based on on-line monitoring of the structural health of components could allow longer intervals between scheduled inspections, or even revolutionize the concept of on-condition maintenance, by making inspections virtually continuous, without any downtime.

Thus, structural health monitoring [4] is a desired feature of new-generation helicopters to reduce the need of costly periodic inspections (which cause about 25% of operating costs [5]), to increase life of components, to reduce downtime due to unscheduled maintenance [6] and to increase in-flight safety, since it has been estimated that about 3% of helicopter accidents are caused by failure in the rotor system [7]. An early warning might be also crucial in slowing down crack propagation with appropriate piloting actions (it has been estimated that

a reduction of 20% of flight speed reduce up to 50% propagation velocity [8]). Moreover, it can help in extending the life of aging helicopters [9].

Although the potential benefits of placing sensors on rotors are very clear, several issues regarding the optimal sensors positioning and powering remain still open. The positioning is a crucial aspect in that it has to be a trade-off between the need of improving the devices performances and reducing the risks of accidental breaks during manufacturing or operational life, and the need of avoiding bonding delamination (see [10] for a complete review of technological issues in the case of wind turbines). The definition of the most efficient way of powering and connecting the sensors is a critical aspect too, due to the need of transmitting power between two frames in relative motion (*i.e.*, between the rotating and the non rotating one) [11]; in the FLITE-WISE EU research project (`http://cordis.europa.eu/project/rcn/108855_en.html`) this problem has been addressed with the use of inductive energy transfer from the fixed to the rotating frame, obtaining power in the order of hundreds of mW. In other projects, alternative ways of devices powering have been explored, for example exploiting vibrational energy harvesting (ARTIMA `http://cordis.europa.eu/project/rcn/72783_en.html`, ADVICE `http://cordis.europa.eu/project/rcn/79966_en.html` and TRIADE `http://cordis.europa.eu/project/rcn/90081_en.html`). These observations highlight the criticalities in using a large number of sensors in rotor health monitoring, in that they require a significant amount of power in conjunction with the need of processing a huge amount of data. Furthermore, the complex aeroelastic behavior of helicopter rotors (due to the high flexibility of the blades, the complex aerodynamic environment in which they operate, the strong aeroelastic couplings, and the unsteady loads acting on them) make the use of techniques developed for rotating machinery and in other field of engineering rather difficult [12]. Consequently, most of the non-destructive damage detection techniques in use in the rotorcraft field are carried out in dedicated facilities, and rely upon visual or localized experimental methods such as acoustic or ultrasonic methods, radiography, X-ray or thermal field methods, which require an approximate knowledge of the dam-

age location as well as its accessibility [13]. On the other hand, considering in-flight monitoring, although a wide range of health and usage monitoring systems (HUMS) are currently available and installed on several helicopters [6], structural health monitoring (SHM) systems aimed at real-time damage identification are still immature for their application in production helicopters. This is mainly due to the difficulty in identifying reliable criteria for damage identification, avoiding false positives and negatives. Due to the real-time nature of SHM, this problem is much more a concern than for usage-based systems, for which however it is also present [14, 15]. The approaches proposed during the years for rotor health monitoring are based upon the comparison of the structure vibratory behavior (namely strain, deflections, natural frequencies, mode shapes and modal damping with respect to their reference values), or upon the analysis of the loads transmitted to the fuselage, exploiting the fact that, in a steady flight, a healthy rotor filters all the load harmonic content from blades except that at frequencies multiple of the number of blades times the rotor angular velocity [16] (*i.e.*, for a four-bladed rotor, only the mean, 4Ω, 8Ω and so on). The presence of other frequencies in the hub load spectrum (especially the larger Ω, commonly referred as 1/rev) highlights some type of unbalance between the blades, potentially due to a damage. The latter approach, that is the most common, is often pursued through the use of track and balance sensors in the hub frame [17, 18, 19], which make difficult the identification of the damage type and its localization (also at a rather coarse level, such as simply identifying the damaged blade). On the other hand, blade natural frequency variation has been proposed in [20] as the parameter identifying blade damage. Furthermore, in [12, 21], several blade alteration types, including mass variation, misadjusted pitch link and damaged trailing edge flaps have been simulated using the comprehensive aeromechanics analysis software CAMRAD [22]. The corresponding aeroelastic responses have been processed on the basis of different criteria (tip displacements and hub loads variation), to assess the most suited approach for each type of damage. These works evolved in a subsequent research aimed at improving damage detection algorithms, both in terms of damage identification

and localization, by exploiting neural networks and fuzzy logic [23, 24, 25, 2], whereas other works investigated the use of a Kalman filter with the aim of removing the training phase, essential in neural-networks and fuzzy-logic based methods[26].

Following the approach introduced in [27, 28, 29], in this work the authors propose a technique for rotor damage detection based on the comparison of differential strain measurements from a limited number of sensors located on different blades. The proposed health monitoring system, following the criteria of multi-purpose sensors, can be also used for blade balancing and real-time blade shape sensing (that can provide useful data to the automatic flight control systems to improve performance and control authority) [30]. Keeping low the number of sensors reduces the complexity to power the system, as well as of data processing and transmission (both requiring power as well). Furthermore, due to both the low cost and reduced weight of the needed instrumentation, their range of applicability can be extended also to lightweight helicopters, whose overall safety level could be significantly improved.

The proposed SHM algorithms are numerically tested on a BO105-inspired main rotor, simulated through the multibody dynamics solver MBDyn[31] (`http://www.mbdyn.org/`, last accessed November 2017), to easily model blade faults. This is a common approach for rotorcraft applications [12] in order to overcome the lack of databases of damaged system responses, as a consequence of the impossibility to fly with damaged blades. Indeed, although it is possible to test damaged blades on whirl tower at a relevant cost (both for infrastructure and blade sets), these tests are unable to reproduce load conditions characteristic of the whole flight envelope, in that it is only suited for structural and aeromechanical analyses of hovering rotors [32].

2. Structural Health Monitoring Algorithms

Despite the differences, in terms of measured quantities and data post-processing techniques used to predict and locate a damage, different SHM al-

gorithms present some common features [33, 34, 35, 36, 37]: i) a reference state is necessary to compare the degraded performance with; ii) high frequency phenomena can pinpoint more accurately the location of the damage; iii) the need of distinguishing between abnormal variation of structural behavior due to damages and natural variation due to external inputs. Thus, helicopter rotors are a favorable field of application, due to the presence of multiple (ideally identical) blades experiencing similar (virtually the same in steady flight conditions) low- to high-frequency excitation with a very small phase shift between them. Considering the classical classification of SHM algorithms in model-driven and data-driven ones, in this work the authors propose a blended approach, which moves from strain based measurements processed taking into account the aforementioned peculiarities of the rotor dynamics.

In this paper, three criteria for the blade damage detection based on the comparison of signals from sensors located on different blades are proposed, and investigated in terms of: i) sensitivity to structural modifications; ii) proneness to false positives and negatives due to unsteady flight conditions.

2.1. Autocorrelation criterion

The first criterion proposed is based on the autocorrelation of the signals obtained as the difference between strain measurements from sensors in the same position on i-th and j-th blades (Δ-signals), namely [38]

$$c_{ij}(\tau) = \frac{1}{T}\int_{-T/2}^{T/2} \Delta s_{ij}(t)\Delta s_{ij}(t+\tau)d\tau \tag{1}$$

Note that, in the absence of a blade damage/imbalance among the blades, the steady-state aeroelastic responses do not differ, once the signals from the blades are phased by their relative angles ($2\pi(i-j)/N_b$). Then, since the difference between two undamaged blades (assumed identical) contains only noise and transient response effects, it is expected that, considering a sufficiently long sampling period, the normalized autocorrelation will be very low, except for zero time shift. On the contrary, when one Δ-signal involves a damaged blade, it becomes strongly periodic and then the autocorrelation will be higher also

for other values of the time shift, as it may be easily verified for two periodic analytical signals.

2.2. Mean and power spectral density criteria

The last two criteria proposed are based on the evaluation of mean and Welch's power spectral density [39] of Δ-signals. Indeed, the power spectral density of each blade response is characterized by contributions at frequencies $n\Omega$ (where Ω is the rotor angular velocity and $n \in \mathbb{N}$), due to steady-periodic response, and $\omega \pm n\Omega$ (where ω is a generic blade eigenfrequency), due to transient response. Since the rotor natural frequencies are separated by design from multiples of the rotor angular velocity in order to avoid resonance, monitoring $n\Omega$ peaks in the blade response is expected to be a suitable criterion for damage identification. In fact, the amplitudes of the PSD peaks of the signals obtained as the difference between strain measurements from different blades (Δ-signal), at frequencies $n\Omega$, are expected to be persistent in time in damaged systems, as opposed to the peaks associated with the transient response of an undamaged system (usually strongly dependent on lightly damped lag modes), which are expected to show a pronounced time dependence. This approach presents several advantages with respect to other approaches in the frequency domain based upon the monitoring of changes in natural frequencies. In particular, it is well known [37] that natural frequencies are relatively insensitive to changes in structural properties, making a damage early detection rather difficult. Furthermore, frequency-domain approaches based on modal shape analysis [40, 41] require a larger set of measurement points, increasing cost, complexity, and power supply issues [37].

Notice that actual blades may differ as a result of the manufacturing process. Dissimilarities are mitigated and maintained within acceptable tolerances by tracking and balancing. Consequently, a non-zero Δ-signal may be present also in undamaged systems, resulting in the rise of hub loads at low multiples of

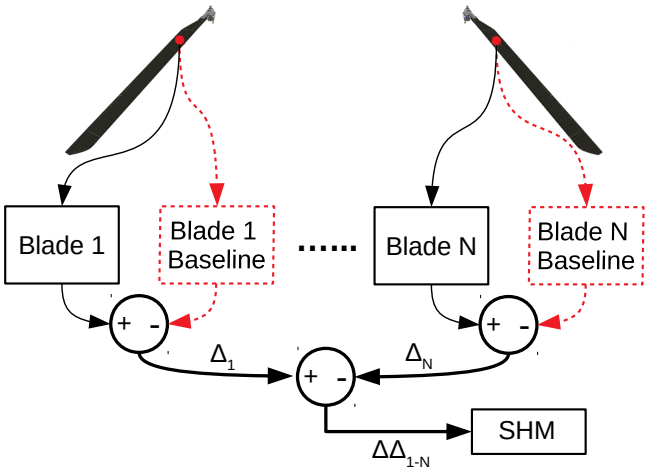

Figure 1: Sketch of $\Delta\Delta$-signals evaluation

Ω (especially 1/rev, which is considered unacceptable above 0.30 ips [12]). To overcome the consequent risk of false positives, all the proposed criteria are applied to the signal

$$\Delta\Delta s_{ij}(t) = \Delta s_{ij}(t) - \Delta s_{ij}^{\mathrm{ref}}(t) \tag{2}$$

namely, the variation of the Δ-signal with respect to the reference state, and referred to as the $\Delta\Delta$-signal in the following (Figure 1 sketches the $\Delta\Delta$-signals evaluation procedure). In practice, the characterization of the reference state requires a sort of calibration process aimed at recording the Δ-signals between different blades, after the track and balance procedure, in different steady flight conditions. Note that, since the blade response depends on several parameters (like flight level and weight) which cannot be considered all in the calibration process, the $\Delta\Delta$-signals may be not exactly zero also for healthy blades. However, if a blade suffers a damage, it is expected to notice a significant increase of the $\Delta\Delta$-signals related to that blade, which is expected to be easily recognizable from the previous situation. Anyway, a relatively large database of baseline flight conditions would be beneficial to improve the accuracy of the health monitoring system.

Note that all the proposed criteria are related to the approaches based on

the analysis of the loads transmitted to the fuselage [12], because the rise of other harmonics with respect to the multiple of the blade passing frequency (BPF, equal to number of blade times rotor angular velocity) implies different blades response. They are also somewhat related to the techniques based on the detection of discrepancies on tip deflection measurement [12], since the latter are caused by a different distribution of deformation/strain. However, the measurement of strain on the blades presents some advantages: i) with respect to hub loads measurements, it does not require complex three-dimensional load cells. Moreover, it easily detects the damaged blade, whereas such identification is impossible from hub loads data, without additional measurements; ii) with respect to tip displacement measurements, it is a quite accurate and easier measurement. Indeed, the blade of a mid-weight helicopter undergoing flap bending resulting in a linear strain distribution with maximum at blade root equal to the typical sensitivity of a modern strain gauge (1 $\mu\varepsilon$) will undergo a tip deflection of less than one third of millimeter. Furthermore, it is worth recalling that direct tip deflection measurement is a complex task, owing to the need of placing cameras in the fixed frame [9].

Considering the three typical performance targets of a Health and Usage Monitoring System (HUMS) [9], namely *detection*, *diagnostic* and *prognostic*, it can be stated that a high sensitivity helps in identifying the insurgence of a damage before it reaches an intolerable level (improving *detection* but also *prognostic* if a proper model of damage progression is available) and measuring directly on the blade helps in damage localization (*diagnostic*), as discussed earlier.

3. Results

The test case considered is a four-blade hingeless rotor inspired to the main rotor of the Bölkow (now Airbus Helicopters) BO105 helicopter, having a radius of 4.9 m, rotating at 44.4 rad/s, focusing on a forward-flight condition at

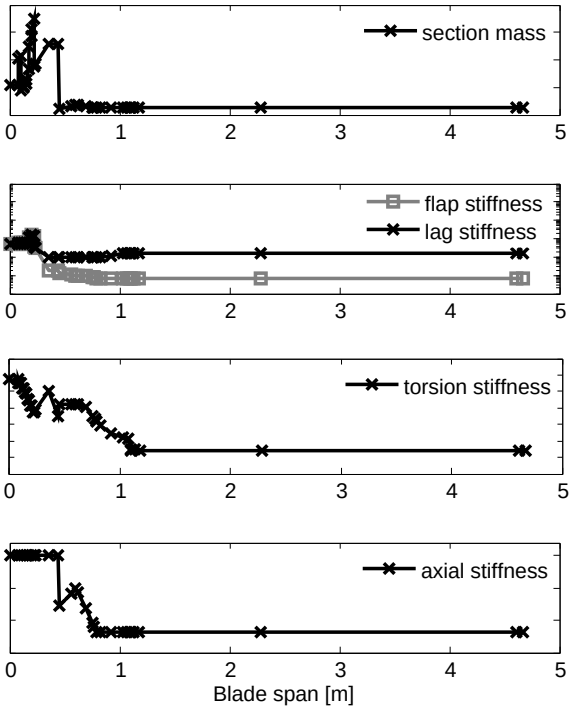

Figure 2: Structural properties distribution.

an advance ratio (the ratio between the forward velocity, V_∞, and the blade tip velocity in hover, ΩR) $\mu = 0.2$. The blades present a realistic spanwise variability of the structural properties. Figure 2 illustrates the trend of the main structural properties along the blade.

Only one strain measurement, collocated in $r^* = 0.1R$ at the chordwise station of each blade elastic axis and aligned with the blade axis itself is considered. Although a detailed investigation on the sensor optimal positioning and orientation is envisaged in the future, here, they have been driven by simple consideration on signal to noise ratio, which is maximum near the root just outside the stiffest region, and on the maximum sensitivity direction of the strain to the blade damages, in that the blade elastic response is strongly dominated by the flapping motion. The actual measurements on the rotor blades are computed from dynamic and aeroelastic simulations performed by the free, general

purpose multibody dynamics solver MBDyn [31].

The rotor blades dynamics is modeled by using the so-called geometrically exact nonlinear beam finite elements [42]. The aerodynamic loads are obtained from the blade element/momentum theory [43], with a Glauert-like linearly distributed static inflow model [43]. The strains are evaluated from the beam displacements using the nonlinear relations proposed in [44], which differ from the classical linear expressions in that valid for moderate displacements, a fundamental requirement in blade structural dynamics analyses. Considering the strain tensor $\boldsymbol{E}$ associated with the stress state that characterizes the beam model simulating the helicopter blade,

$$\boldsymbol{E} = \begin{bmatrix} \varepsilon_{\xi\xi} & \varepsilon_{\xi\eta} & \varepsilon_{\xi\zeta} \\ \varepsilon_{\xi\eta} & -\nu\varepsilon_{\xi\xi} & 0 \\ \varepsilon_{\xi\zeta} & 0 & -\nu\varepsilon_{\xi\xi} \end{bmatrix} \tag{3}$$

where the ξ axis is tangent to the elastic axis, whereas the η and ζ axes are the cross-section principal axes, the strain-displacement relation reads

$$\begin{aligned} \varepsilon_{\xi\xi} = {} & u' + \frac{1}{2}(v'^2 + w'^2) - \lambda\varphi'' \\ & + (\eta^2 + \zeta^2)\left(\vartheta'\varphi' + \frac{\varphi'^2}{2}\right) \\ & - v''[\eta\cos(\vartheta+\varphi) - \zeta\sin(\vartheta+\varphi)] \\ & - w''[\eta\sin(\vartheta+\varphi) + \zeta\cos(\vartheta+\varphi)] \end{aligned} \tag{4a}$$

$$\varepsilon_{\xi\eta} = -\frac{1}{2}\left(\zeta + \frac{\partial\lambda}{\partial\eta}\right)\varphi' \tag{4b}$$

$$\varepsilon_{\xi\zeta} = \frac{1}{2}\left(\eta - \frac{\partial\lambda}{\partial\zeta}\right)\varphi' \tag{4c}$$

where u, v, and w are the axial, lead-lag and flap displacements of the elastic axis, $'$ indicates the derivative with respect to the ξ coordinate, ϑ is the built-in twist angle, φ is the blade cross-section elastic torsion, and λ is the section warping function.

Two types of alteration on the blade are analyzed: (i) variation in mass; (ii) variation in flapwise stiffness;

The mass alteration consists in a lumped mass at the tip of blade #1. Rather than introducing a very short beam element, the structural damage in a region of length $L_d \ll R$ centered at $\overline{r}$ producing a flapwise stiffness reduction is simulated by dividing the blade into two beams connected in $\overline{r}$ by a rotational joint that allows relative flapwise rotation, restrained by a spring of stiffness K that reproduces the yielding at the damage location. Considering the case of flapwise bending stiffness variation (analogous considerations may be made for lead-lag and torsion), the spring constant is evaluated by considering the equivalence in terms of flapping bending angle along the entire degraded blade trait, namely

$$\int_{\overline{r}-\frac{L_d}{2}}^{\overline{r}+\frac{L_d}{2}} \frac{M}{S_d} dx = \int_{\overline{r}-\frac{L_d}{2}}^{\overline{r}^-} \frac{M}{S_u} dx + \Delta w' + \int_{\overline{r}^+}^{\overline{r}+\frac{L_d}{2}} \frac{M}{S_u} dx \tag{5}$$

where, S_u and S_d are the undamaged and damaged blade stiffness, respectively. Then, assuming the bending moment M to be constant along the damaged zone and equal to that exerted by the spring, Equation (5) is solved to obtain the equivalent spring constant

$$K = \frac{\dfrac{1}{L_d}}{\dfrac{1}{S_d} - \dfrac{1}{S_u}} \tag{6}$$

One can easily show that under the same assumption on bending moment M, and neglecting shear strain (*i.e.*, using Kirchhoff's kinematic model), the transverse displacement is preserved when the equivalent lumped spring is considered.

3.1. Time-domain analysis

The first results presented show the autocorrelation of the $\Delta\Delta$-signal over 100 revolutions. Note that, although the undamaged blades are nominally identical, the numerical solution of the aeroelastic simulation introduces systematic discrepancies in the blade response. Thus, even here the use of the $\Delta\Delta$-signal instead of the Δ-signal is beneficial. Notice that modern strain gauges have very high strain resolution (up to the nano-epsilon range) and thus the numerical

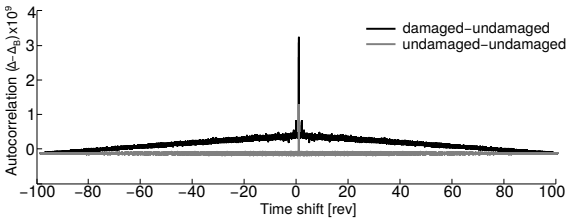

Figure 3: Autocorrelation of $\Delta\Delta$-signal from altered (+2 g @tip) and nominal blades.

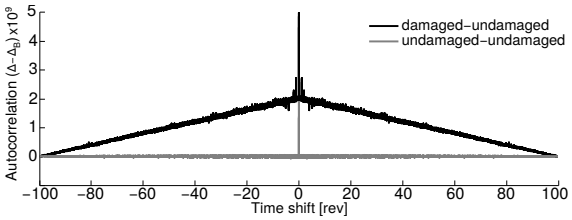

Figure 4: Autocorrelation of $\Delta\Delta$-signal from altered (+4 g @tip) and nominal blades.

errors are representative of a real-life application, where noise and systematic errors are always present. Figures 3 and 4, which show the autocorrelation of the $\Delta\Delta$-signal, clearly show the effect of adding a mass of 2 and 4 grams, respectively, at the tip of one blade. The almost triangular shape of *damaged-undamaged* curves anticipates the preeminence of mean value on $\Delta\Delta$-signals, as it will be made clearer from the following analyses.

Figure 5 shows what happens if the autocorrelation is performed over the Δ-signal instead of the $\Delta\Delta$-signal. When the Δ-signal is used, the damaged blade is no longer recognizable in the case of 2 grams tip mass alteration, in that the autocorrelation of undamaged blades presents a triangular behavior, as well. Figure 5 shows four groups of curves resulting from the Δ-signals among all blades. The same curves, although related to $\Delta\Delta$-signals, are also shown in Figures 3 and 4; however, thanks to the fact that the $\Delta\Delta$-signals hide the inevitable small differences among the blades when undamaged, in those cases the *undamaged-undamaged* curves are indistinguishable, as well as the *damaged-undamaged* ones.

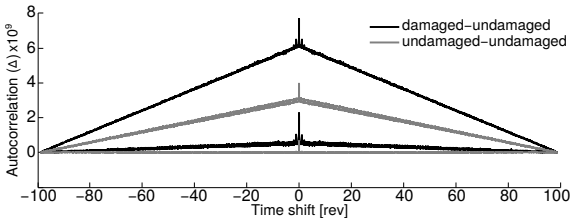

Figure 5: Autocorrelation of Δ-signal from altered (+2 g @tip) and nominal blades.

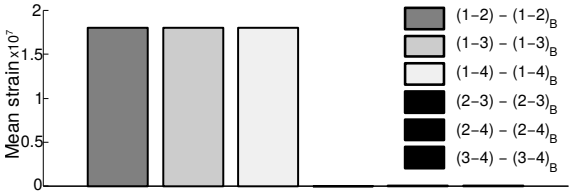

Figure 6: Mean value of ΔΔ-signal from altered (+2 g @tip) and nominal blades.

Although the systematic discrepancy between undamaged blades is a purely numerical problem, it is expected that an analogous situation will be present in real-life cases, making the use of the ΔΔ-signal an interesting means to make the analysis more robust. Complementary information may be drawn from the analysis of the mean value of ΔΔ-signals, shown in Figures 6 and 7 for 2 and 4 grams tip mass, respectively. The presence of blade damage clearly appears in all the bars involving blade 1 (the damaged one), with an almost identical effect. On the contrary, the mean value of ΔΔ-signals between undamaged blades are more than two orders of magnitude smaller. Figure 8 shows an example of mean value analysis considering Δ-signals instead of ΔΔ-signals. As noted before, also in this case the damaged blade is not clearly recognizable. Note that the considered mass alteration produces a ΔΔ-signal which is slightly smaller than commercial FBG strain sensors resolution (which is about $1\,\mu\varepsilon$)

Figures 9 to 12 show autocorrelation and mean value of ΔΔ-signals in presence of damage which respectively causes a 5% or 10% flapwise stiffness reduction on a 1 cm long portion of blade positioned at $\overline{r} = 0.33R$, leading to considerations analogous to those made for the additional mass.

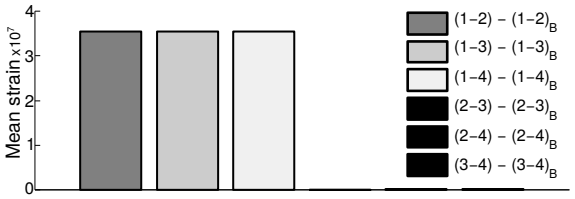

Figure 7: Mean value of $\Delta\Delta$-signal from altered (+4 g @tip) and nominal blades.

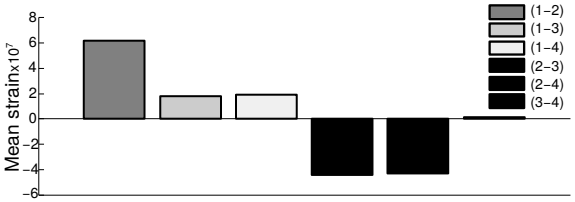

Figure 8: Mean value of Δ-signal from altered (+2 g @tip) and nominal blades.

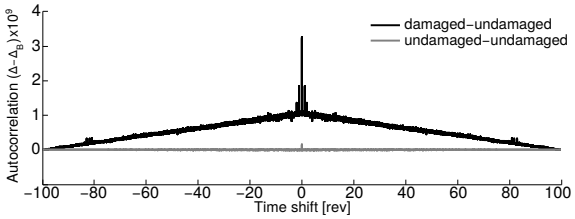

Figure 9: Autocorrelation of $\Delta\Delta$-signal from altered (5% flapping stiffness reduction on 1 cm @$r = 1.53$ m) and nominal blades.

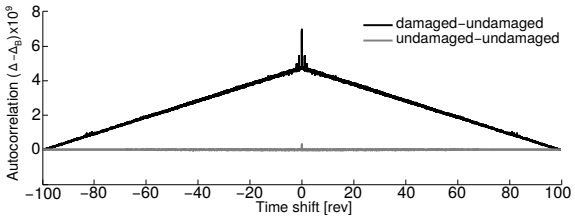

Figure 10: Autocorrelation of $\Delta\Delta$-signal from altered (10% flapping stiffness reduction on 1 cm @$r = 1.53$ m) and nominal blades.

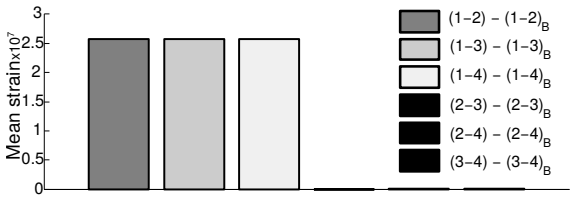

Figure 11: Mean value of $\Delta\Delta$-signal from altered (5% flapping stiffness reduction on 1 cm @$r = 1.53$ m) and nominal blades.

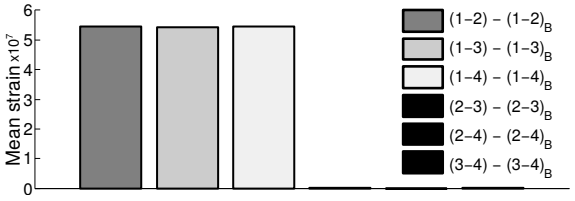

Figure 12: Mean value of $\Delta\Delta$-signal from altered (10% flapping stiffness reduction on 1 cm @$r = 1.53$ m) and nominal blades.

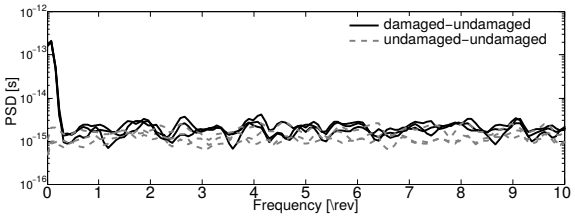

Figure 13: PSD of $\Delta\Delta$-signal from altered (+2 g @tip) and nominal blades.

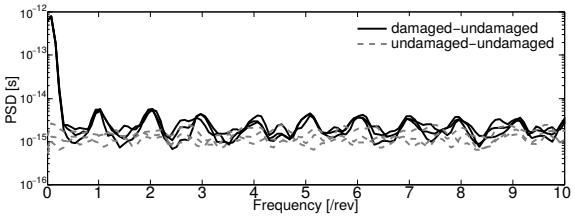

Figure 14: PSD of $\Delta\Delta$-signal from altered (+4 g @tip) and nominal blades.

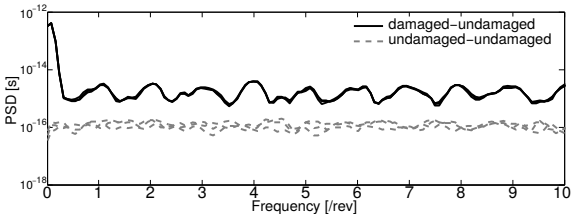

Figure 15: PSD of $\Delta\Delta$-signal from altered (5% flapping stiffness reduction on 1 cm @$r = 1.53$ m) and nominal blades.

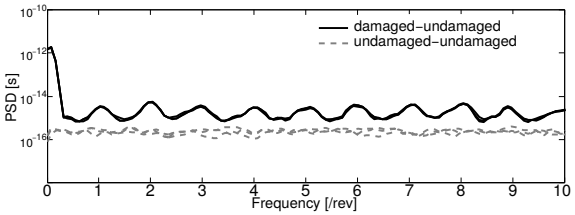

Figure 16: PSD of $\Delta\Delta$-signal from altered (10% flapping stiffness reduction on 1 cm @$r = 1.53$ m) and nominal blades.

3.2. Frequency-domain analysis

The same damaged configurations are investigated also using the frequency domain approaches presented in Section "Structural Health Monitoring Algorithms". Figures 13 and 14 show the PSD of the $\Delta\Delta$-signal in presence of 2 grams and 4 grams of additional mass at the tip of blade #1, respectively. The PSDs have been obtained through Welch's algorithm using a 100-revolutions long signal, divided in 10 Blackman-Harris windowed chunks with 50% overlap. As expected, a great discrepancy can be observed at zero frequency between the PSDs of $\Delta\Delta$-signals involving the damaged blade and those not involving it. Moreover, the PSDs also highlight other discrepancies of the forced (periodic) response at frequency Ω, 2Ω, ..., $N\Omega$.Peaks at $n\Omega$ are clearly visible in Figure 14, whereas in Figure 13 the type and entity of the damage hide this behavior.

When considering the flapwise stiffness reduction (see Figures 15 and 16), the $n\Omega$ peaks are present also for a small damage, along with the peak at zero

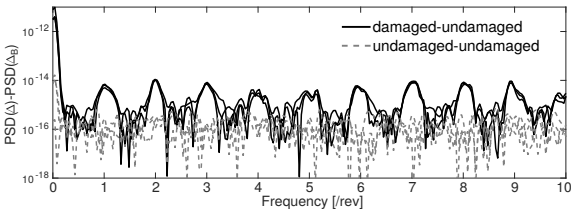

Figure 17: Δ-PSD of Δ-signal from altered (10% flapping stiffness reduction on 1 cm @$r = 1.53$ m) and nominal blades.

frequency. This is probably due to the fact that this kind of alteration affects modes having frequency higher than those affected by the addition of a tip mass.

In order to reduce the requirements in terms of data storage, in practical applications, a slightly modified algorithm can be used. Specifically, it is based upon the evaluation of the difference of the PSD of the Δ-signals (Δ PSD(Δ-signals)) instead of the evaluation of the PSD of the ΔΔ-signals. This procedure allows to store only the PSD of baseline signals up to the frequency of interest, without the need of storing long signal time histories too. Figure 17 shows that this second criterion, although not completely equivalent to the previous one owing to the nonlinearity of the PSD, for the same case of Figure 16 yields results that are more noisy but of similar quality.

3.3. Algorithms performance in maneuvered flight

To assess the effect of maneuvered flight on damage detectability, two simple excitations have been imposed to the rotor in steady flight. They consist of two $1 - \cos$ collective doublets, separated by 4 s (about 28 rotor revolutions) and characterized by $\pi/2$ and $\pi/4\,\mathrm{rad\,s^{-1}}$ frequency and 0.5° and 0.6° amplitude, respectively. These perturbations produce thrust variation of about ±20% with respect to the leveled flight value. In this case, owing to the periodicity of rotor dynamics in forward flight, the aeroelastic responses differ also between undamaged blades. Considering the 10%-damage case analyzed before, Figure 18 clearly shows the effect of the excitation on Δ-signals in terms of forced and free response, the latter mainly driven by the low-frequency lead-lag and flap modes.

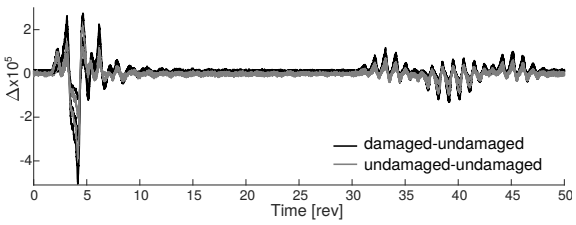

Figure 18: Δ-signals in response to collective excitation.

Note that, the first lead-lag mode is very lightly damped, causing the long halving time. Figure 19 shows the autocorrelation of ΔΔ-signals for the same case. The beats appearing at about ±35 rev and ±5 rev time shifts are associated with the periodic signals caused by the response to the collective excitation. Although the autocorrelations from undamaged blades also exhibit some beats, two significant considerations may be drawn: i) the amplitude of the beats is significantly larger in relation with damaged blades; ii) the autocorrelation of signals between undamaged blades show an almost flat mean trend, whereas the signals involving the damaged blade present the characteristic triangular shape (although partially hidden by the figure scale) mentioned before.

The differences are more evident in Figure 20, where the two sets of signals (those involving the damaged blade and those not involving it) have been summed together (ΣΔΔ-signals). It is worth noticing that this operation may also define an alternative criterion, given that it should be repeated for all the possible combinations of blade sets, unless one knows which the damaged blade is. After defining "pivotal element" the blade index that always appears in the first set and never appears in the second one (blade number 1 in Figure 20), only the analysis performed with the damaged blade as the pivotal element would exhibit a significant discrepancy between the two sets.

Considering the mean value and frequency domain analysis criteria, the presence of the excitation makes the discernment more complicated but still feasible. The mean value criterion (Figure 21) remains highly predictive, whereas the PSD of the ΔΔ-signals (Figure 22) becomes less sharp, especially above the

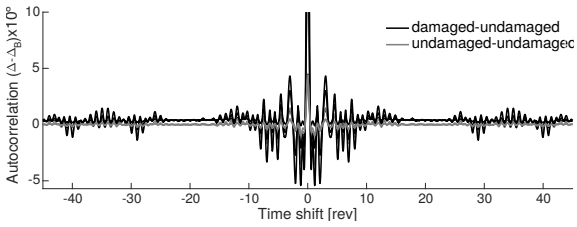

Figure 19: Autocorrelation of $\Delta\Delta$-signal in presence of collective excitation.

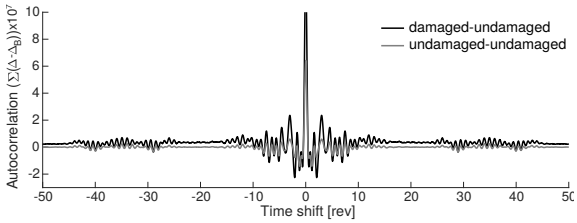

Figure 20: Sum of autocorrelations of $\Delta\Delta$-signal in presence of collective excitation.

2/rev frequency. Moreover, as expected from Figure 18, there are significant peaks in the low-frequency range (up to 2/rev), which are caused by the collective input and the subsequent free response. In fact, the latter is dominated by the low-frequency blade lead-lag and flap modes (respectively slightly below and slightly above 1/rev). However, also in this region the $\Delta\Delta$-signals involving the damaged blade are on average greater.

Finally, the Δ-PSDs of the sum of Δ-signals are shown in Figure 23. Here, noticeable differences are present also above 3/rev, although much less pronounced than in the steady flight case.

In order to reduce the problems caused by unsteady phenomena during flight, the exclusion of strain data coming from strongly maneuvered flight sections (for instance discerned through c.g. acceleration rms) is advisable. This should not represent a big issue, since flight is usually characterized by long almost steady flight periods.

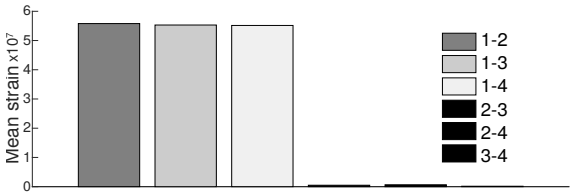

Figure 21: Mean value of $\Delta\Delta$-signal in presence of collective excitation.

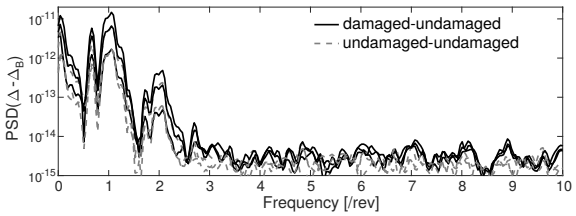

Figure 22: PSD of $\Delta\Delta$-signal in presence of collective excitation.

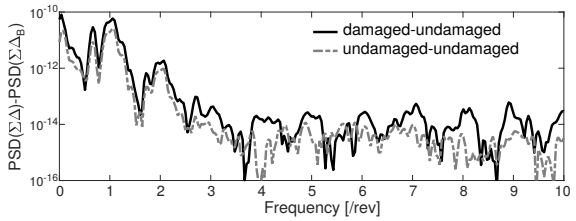

Figure 23: ΔPSD of the sum of Δ-signal in presence of collective excitation.

4. Conclusions & future work

The structural health monitoring of helicopter blades has been addressed using both frequency and time domain analyses applied on the difference of strain signals (Δ-signals) among rotor blades. Although here they rely only on one measurement point for each blade, the techniques may be applied to the same measurements used for shape sensing, an asset in view of an integrated instrumentation lodged on the rotor head. Moreover, these techniques may be conveniently applied to wind turbine rotors, for which continuous, long term operations are required and the choice of the right maintenance time is crucial for minimizing the Cost of Energy (CoE).

The different techniques showed the capability to detect blade mass or stiffness alterations, even of small entity, as well as the ability of easily identifying the damaged blade. The use of a reference Δ-signal (to address the differences among blades caused by fabrication process) is promising in order to reduce false positives. Preliminarily, all the proposed techniques have shown to be inherently lowly affected by random noise (being based on relatively long period of acquisition); furthermore, the comparison with the baseline signal is also aimed at minimizing the effect of systematic measurement errors. The accuracy and robustness during maneuvered flight in presence of external disturbance has been addressed as well, coming to the conclusion that strong maneuvers worsen the accuracy of the autocorrelation and PSD criteria for damage detection, whereas mean value criterion turned out to be more robust. Due to this, in practical applications the signal analysis should be limited to steady or quasi-steady flight periods.

Many future investigations may be envisaged: i) assessment of the need of a database of reference Δ-signals for various flight conditions. In particular the feasibility of such a database has to be assessed, since previous attempts to build one in terms of signals only had partial success. ii) a more systematic analyis of the effect of the measurement noise on the SHM algorithm performance iii) use of a network of sensors instead of only one sensor for each blade and the devel-

opment of data fusion algorithms, also for reducing the effects of measurement errors; iv) the use of different time-frequency transformations, like the wavelet transform; v) the use of machine learning/deep learning algorithms to identify damage characteristic patterns in the damage indicators proposed in the present paper.

References

[1] W. Johnson, Rotorcraft Aeromechanics, Cambridge University Press, 2013.

[2] P. M. Pawar, R. Ganguli, Structural health monitoring of composite helicopter rotor, in: Structural Health Monitoring Using Genetic Fuzzy Systems, Springer, 2011, pp. 85–125.

[3] VV.AA., Certification specifications for small rotorcraft, Tech. rep., European Aviation Safety Agency (2012).

[4] C. R. Farrar, K. Worden, An introduction to structural health monitoring, Philosophical Transactions of the Royal Society of London A: Mathematical, Physical and Engineering Sciences 365 (1851) (2007) 303–315.

[5] J. D. Cronkhite, Practical application of health and usage monitoring (hums) to helicopter rotor, engine, and drive systems, in: Annual Forum Proceedings-American Helicopter Society, Vol. 49, American Helicopter Society, 1993, pp. 1445–1445.

[6] P. Pawar, R. Ganguli, Helicopter rotor health monitoring-a review, proceedings of the institution of mechanical engineers, part G: Journal of Aerospace Engineering 221 (5) (2007) 631–647.

[7] L. Iseler, J. De Maio, An analysis of us civil rotorcraft accidents by cost and injury (1990-1996), Tech. Rep. TM-2002-209615, NASA (2002).

[8] H. Le Sueur, Airworthiness of helicopters, The Aeronautical Journal 82 (814) (1978) 411–416.

[9] P. W. Stevens, D. Hall, E. Smith, A multidisciplinary research approach to rotorcraft health and usage monitoring, in: Proc. Annual Forum, American Helicopter Society, Vol. 2, 1996, pp. 1732–1751.

[10] S.-W. Kim, W.-R. Kang, M.-S. Jeong, I. Lee, I.-B. Kwon, Deflection estimation of a wind turbine blade using fbg sensors embedded in the blade bonding line, Smart Materials and Structures 22 (12) (2013) 125004.

[11] A. Sanchez Ramirez, R. Loendersloot, T. Tinga, Helicopter rotor blade monitoring using autonomous wireless sensor network, Key engineering materials 569 (2013) 775–782.

[12] R. Ganguli, I. Chopra, D. J. Haas, Formulation of a helicopter rotor system damage detection methodology, Journal of the American Helicopter Society 41 (4) (1996) 302–312.

[13] S. W. Doebling, C. R. Farrar, M. B. Prime, et al., A summary review of vibration-based damage identification methods, Shock and vibration digest 30 (2) (1998) 91–105.

[14] J.-M. Poradier, M. Trouvé, An assessment of eurocopter experience in hums development and support, in: IN: AHS International Annual Forum, 57 th, Washington, DC, May 9-11, 2001, Proceedings(A 02-12351 01-05), Alexandria, VA, AHS International, 2001, 2001.

[15] M. Augustin, S. Bradley, Achieving hums benefits in the military environment–hums developments on the ch-146 griffon fleet, in: American Helicopter Society 60th Annual Forum, 2004.

[16] R. L. Bielawa, Rotary wing structural dynamics and aeroelasticity, American Institute of Aeronautics and Astronautics Washington, DC, 1992.

[17] M. Andrew, The diagnosis of helicopter main rotor faults, in: Proceedings of the 9th European Rotorcraft Forum, 1983.

[18] A. Rosen, R. Ben-Ari, Mathematical modelling of a helicopter rotor track and balance: theory, Journal of Sound and Vibration 200 (5) (1997) 589–603.

[19] R. Ben-Ari, A. Rosen, Mathematical modelling of a helicopter rotor track and balance: results, Journal of sound and vibration 200 (5) (1997) 605–620.

[20] H. Azzam, M. Andrew, The use of math-dynamic models to aid the development of integrated health and usage monitoring systems, Proceedings of the Institution of Mechanical Engineers, Part G: Journal of Aerospace Engineering 206 (1) (1992) 71–76.

[21] R. Ganguli, I. Chopra, D. J. Haas, Simulation of helicopter rotor-system structural damage, blade mistracking, friction, and freeplay, Journal of aircraft 35 (4) (1998) 591–597.

[22] W. Johnson, CAMRAD II, Comprehensive Analytical Model of Rotorcraft Aerodynamics and Dynamics, Analytical Methods, Inc, 1982.

[23] R. Ganguli, I. Chopra, D. J. Haas, Detection of helicopter rotor system simulated faults using neural networks, Journal of the american helicopter society 42 (2) (1997) 161–171.

[24] R. Ganguli, I. Chopra, D. J. Haas, Helicopter rotor system fault detection using physics-based model and neural networks, AIAA journal 36 (6) (1998) 1078–1086.

[25] R. Ganguli, A fuzzy logic system for ground based structural health monitoring of a helicopter rotor using modal data, Journal of Intelligent Material Systems and Structures 12 (6) (2001) 397–407.

[26] J. Alkahe, Y. Oshman, O. Rand, Adaptive estimation methodology for helicopter blade structural damage detection, Journal of Guidance Control and Dynamics 25 (6) (2002) 1049–1057.

[27] C. Enei, G. Bernardini, J. Serafini, L. Mattioni, C. Ficuciello, V. Vezzari, Photogrammetric detection technique for rotor blades structural characterization, in: Journal of Physics: Conference Series, Vol. 658, IOP Publishing, 2015, p. 012003.

[28] G. Bernardini, J. Serafini, C. Enei, L. Mattioni, C. Ficuciello, V. Vezzari, Structural characterization of rotor blades through photogrammetry, Measurement Science and Technology 27 (6) (2016) 065401.

[29] J. Serafini, G. Bernardini, L. Mattioni, V. Vezzari, C. Ficuciello, Non-invasive dynamic measurement of helicopter blades, in: Journal of Physics. Conference Series, Vol. 882, 2017, p. 012014.

[30] G. Bernardini, R. Porcelli, J. Serafini, P. Masarati, Shape sensing and structural health monitoring of rotor blades from strain analysis, in: AHS 73nd Annual Forum & Technology Display, 2017.

[31] P. Masarati, M. Morandini, P. Mantegazza, An efficient formulation for general-purpose multibody/multiphysics analysis, Journal of Computational and Nonlinear Dynamics 9 (4) (2014) 041001, doi:10.1115/1.4025628.

[32] B. P. Ergul, O. Yasa, G. Tursun, Determination of structural integrity of teetering rotor system by whirl tower tests, in: Proceedings of 39th European Rotorocraft Forum, 2013.

[33] S. W. Doebling, C. R. Farrar, M. B. Prime, D. W. Shevitz, Damage identification and health monitoring of structural and mechanical systems from changes in their vibration characteristics: a literature review, Tech. rep., Los Alamos National Lab., NM (United States) (1996).

[34] H. Sohn, C. R. Farrar, F. M. Hemez, D. D. Shunk, D. W. Stinemates, B. R. Nadler, J. J. Czarnecki, A review of structural health monitoring literature: 1996–2001, Los Alamos National Laboratory, USA.

[35] R. B. Randall, State of the art in monitoring rotating machinery-part 1, Sound and vibration 38 (3) (2004) 14–21.

[36] R. B. Randall, State of the art in monitoring rotating machinery-part 2, Sound and Vibration 38 (5) (2004) 10–17.

[37] D. Montalvao, N. M. M. Maia, A. M. R. Ribeiro, A review of vibration-based structural health monitoring with special emphasis on composite materials, Shock and Vibration Digest 38 (4) (2006) 295–326.

[38] J. A. Gubner, Probability and Random Processes for Electrical and Computer Engineers, Cambridge University Press, 2006.

[39] P. Welch, The use of fast fourier transform for the estimation of power spectra: a method based on time averaging over short, modified periodograms, IEEE Transactions on audio and electroacoustics 15 (2) (1967) 70–73.

[40] T. J. Arsenault, A. Achuthan, P. Marzocca, C. Grappasonni, G. Coppotelli, Development of a fbg based distributed strain sensor system for wind turbine structural health monitoring, Smart Materials and Structures 22 (7) (2013) 075027.

[41] F. L. M. dos Santos, B. Peeters, H. Van der Auweraer, L. C. Sandoval Góes, Modal strain energy based damage detection applied to a full scale composite helicopter blade, in: Key Engineering Materials, Vol. 569, Trans Tech Publ, 2013, pp. 457–464.

[42] G. L. Ghiringhelli, P. Masarati, P. Mantegazza, A multi-body implementation of finite volume beams, AIAA Journal 38 (1) (2000) 131–138, doi:10.2514/2.933.

[43] J. G. Leishman, Principles of Helicopter Aerodynamics, Cambridge University Press, Cambridge, UK, 2000.

[44] D. H. Hodges, E. H. Dowell, Nonlinear equation for the elastic bending and torsion of twisted nonuniform rotor blades, Tech. Rep. TN D-7818, NASA (1974).